SLAC-PUB-125
June 1965

PROTON FORM FACTORS FROM PROTON OBSERVATION

D. Frerejacque,† D. Benaksas and D. Drickey‡

Laboratoire de l'Accélérateur Linéaire

Ecole Normale Supérieure

Faculté des Sciences, Orsay, Seine et Oise, France

ABSTRACT

A determination of the electric and magnetic form factors of the proton has been made by studying the elastic sacttering of electrons from a polyethylene target by observation of the recoiling proton at 0° and 30° for values of q^2 between 1 fermi^{-2} and 1.8 fermi^{-2}. From these measurements we have deduced the charge radius R_c and the magnetic radius R_m of the proton and find equality within the experimental errors ($R_c = 0.800 \pm 0.025$ fermi ; $R_m = 0.810 \pm 0.029$ fermi).

(Submitted to The Physical Review)

†Now Scientific Attache, Embassy of France, Washington, D. C.

‡Now at the Stanford Linear Accelerator Center, Stanford University, Stanford, California

I. INTRODUCTION

The study of electron-proton elastic scattering in the range of validity of the first Born approximation leads to the determination of two form factors G_c and G_m, in the Sachs definition.[1]

The most convenient way to achieve their determination is to study the collision for the same value of q^2 in two different kinematic situations. In most experiments[2] this has been done by observing the scattered electron at forward and backward angles. We have performed the complementary experiment, a measurement of the cross sections for the reaction through observation of the recoil proton. This method has some advantages with respect to the other one, namely, the detection of the recoil proton at 0^o leads directly to the determination of $G_m(q^2)$, and the observation of the proton recoiling at another angle leads to $G_c(q^2)$, providing that the value G_m is known for the same value of the square of the four-momentum transfer q^2. Because the experimental techniques are very different, it was hoped that systematic errors would disappear or at least be different for the two types of experiments.

II. FORMULAS

Because the momentum-analyzed recoil proton was detected in a spectrometer, the angle of recoil and the momentum of the elastic proton were used to determine the kinematics rather than the alternative choice of the energy of the incident beam.

Letting M, P and T denote the mass, momentum and kinetic energy of the proton, and γ the recoil angle, the expression for the differential

cross section σ in the laboratory system becomes:

$$\sigma = \frac{B}{\cos} \left(1 + \frac{T}{2M}\right) \frac{2M}{T} \sin^2 \gamma \cdot G_c^2(q^2) + \left[(1 + \cos^2 \gamma)\left(1 + \frac{T}{M}\right) - \frac{2P}{M} \cos \gamma\right] G_m^2(q^2) \quad (1)$$

where

$$B = (e^2/M) = 2.35 \times 10^{-32} \text{ cm}^2$$

and G_c and G_m are the Sachs form factors.[1,2]

The energy of the incident beam is given by

$$E = \frac{MT}{P \cos \gamma - T} \quad (2)$$

The cross section reduces to a very simple form in the case of a recoil at 0^o, allowing direct determination of G_m.

III. EXPERIMENTAL CONDITIONS

A. Experimental Setup

A well collimated beam of electrons of energy between 100 MeV and 160 MeV, produced by the Linear Electron Accelerator located at the Faculté des Sciences de l'Université de Paris, was analyzed in energy by a two-magnet system and passed through a thin target of polyethylene. The protons recoiling elastically were analyzed in momentum by a double-focusing, Judd-type spectrometer set either at zero degrees or at thirty degrees, with the analyzed protons focused on a two-counter telescope. The beam was monitored by a secondary emission monitor (SEM) located either before or after the target. The curves of counting rate versus momentum allowed us to distinguish between the elastic peak of the protons and the continuous background of protons coming from carbon in the target and from other sources. Figures 1 and 2 show the setup in both cases.

B. Determination of the Charge Transported by the Beam

The beam current was measured by using a secondary emission monitor, calibrated frequently, versus a Faraday cup. In the experiments at 30° a standard SEM[3] located after the target was used, while in the 0° experiment the SEM had to be located before the target and as far from the spectrometer as permitted by multiple scattering in order to minimize its contribution to the proton background. It was situated about 1.5 meters from the target and was of the type described in Ref. 4, with a collecting cylinder between two emitting foils each three microns thick. The charge collected by the SEM was measured with a current integrator. Errors in the measurement are due to: (1) error on the efficiency of the Faraday cup (0.995 ± 0.003); (2) error on the capacitors of the integrators; (3) errors on digital voltmeter readings.

Because a low efficiency SEM was used in the 0° experiment, the accuracy of the charge measurement was about 0.32% for the 30° experiments and 0.8% for the 0° experiments.

C. Target

The targets used were foils of CH_2 of thickness chosen between 10 mg/cm^2 and 30 mg/cm^2, depending on the energy of the elastic proton we wished to observe. Chemical analysis has shown no deviation of composition from the stated formula. The foil was fixed in a frame of known area mounted on an oscillating target holder. The oscillation minimized any damage to the target caused by the beam and averaged the irregularities of the target. The plane of the target was parallel to the entry face of the spectrometer, the angle of the target with the beam being accurately measured by the Poggendorf method. We have assigned 0.4% error to the number of protons/cm^2 encountered by the beam.

D. Double-Focusing Spectrometer and Solid Angle

Use of the spectrometer is necessary in order to achieve, by a momentum analysis, an adequate separation between elastic protons and protons coming from electro-disintegration of the target. It is used, in addition, to determine the energy of the elastic protons, thus giving the kinematics of the reaction since the angle is known from the spectrometer position. The calibration has been performed several times by the floating wire method with a reproducibility of 0.5%.

In the experiments done at 30°, the solid angle was defined by a brass slit located outside the fringing field. The choice of the profile of the slit resulted in a penetration correction of the inner edge of less than 0.01%. The absolute value of the solid angle was defined to better than 0.4%.

In the experiment at 0°, both the electron beam and the scattered protons from the target entered the spectrometer. The electrons, deflected downward, were stopped in the magnet at a point which is only slightly dependent on the variation of the field in the spectrometer and consequently on the momentum transfer observed. Some shielding was necessary around the impact point to stop secondary particles from reaching the counters and especially to shield the counters against the big flux of neutrons created.

The solid angle could not be defined by a slit between the target and the spectrometer because of the divergence of the electron beam; we therefore located a slit inside the spectrometer after the impact point of the electrons. At constant field, the solid angle so defined depends on the momentum of the particle analyzed; using first-order theory,[5] we can show that the variation is only 0.25% for a variation of $\Delta P/P = 3\%$. The value of the solid angle so defined was determined by taking the ratio of the counting rate of protons coming from a carbon target with the inner slit to the rate

with an outer slit of known area. The resultant error in the solid angle, mainly due to statistics, was 1%.

E. Detection of Protons

Proton detection was made in two plastic scintillators in coincidence, the second one stopping, or nearly stopping, the protons. The signals given by the photomultipliers were clipped by a 12-cm RG-58-U line (12-ohm clip), which shortened the pulse from 14 nsec to 7 nsec measured at mid-height. This diminished greatly the pile-up caused by the neutron background in the 0^{o} experiment. The electronic logic consisted of Chronetics discriminators and a coincidence unit used with 5 nsec resolving time, with the resultant coincidence pulse used to trigger a pulse height analyzer which stored the pulse coming from the second scintillator. During the setup the spectra in each counter were carefully examined by triggering the pulse height analyzer either with the coincidence or the individual counters, the latter being useful in setting the thresholds of the discriminators. An efficiency of 100% is compatible with the spectra obtained.

IV. CROSS SECTION DETERMINATION

A. Flat-Top Conditions

In order to minimize errors on the cross section, we chose to use the flat-top method, i.e., using a momentum resolution in the spectrometer much larger than the width of the elastic peak. This method, while increasing the backgrounds slightly, has many advantages. In particular, the measurement is essentially independent of the spectrometer dispersion, a quantity difficult to measure accurately. The peak method, although it minimizes backgrounds, leads to a difficult error analysis problem, while the error

assignment is straightforward for the flat-top method.

Previous studies[6] of the double-focusing spectrometer have shown that by reducing sufficiently the entrance aperture, a part of the focal plane corresponding to $\Delta p/p$ of 3.1% can be used with no loss in transmission since the particles travel in aberration-free regions.

If we assume that the elastic peak shape after the radiative tail is subtracted is gaussian, the width at mid-height would be less than $\Delta p/p = 1\%$ in order to have 0.997 or more of the protons in the 3.1% range. Therefore we were forced to minimize the effects contributing to the broadening of the peak in order to measure the true cross section accurately. The main effects are listed below.

1. Effects caused by the finite kinematic of the reaction:
   - Dispersion in energy of the incident electrons
   - Angular divergence of the incident beam
   - Finite horizontal aperture of the spectrometer
   - Finite horizontal size of the beam on the target
   - Finite target length
2. Effects caused by the target:
   - Difference of energy loss between protons arising from collisions on one side or the other of the target
3. Effects caused by the spectrometer:
   - Loss of resolution due to finite vertical size of the beam spot on the target
   - Aberrations of the spectrometer

The most important effects are (2) in a zero-degree experiment and, (2) and (1) in a non-zero degree experiment. Thin targets of polyethylene

set parallel to the entry face of the spectrometer were chosen, and, for the 30° experiment, the horizontal acceptance of the spectrometer was limited to 0.7°.

The curves of the counting rate versus momentum of the proton are shown in Figs. 3 and 4.

B. Modus Operandi

The location of the flat-top was accurately obtained, and counts were accumulated on a point near the middle of the flat-top. The location of the mid-height point at the right of the flat-top was checked often because it is a very sensitive test of the energy stability of the incident beam.

The background under the flat-top was subtracted by measuring with accuracy the background on each side of the peak, subtracting the contribution given by the radiative tail for lower momentum, and then making a polynomial least square fit of the residual background. We feel this method is freer from bias and more precise than the alternative choice of using a carbon target of known thickness as a dummy target.

C. Corrections to the Measurements

Counting rate corrections in the Chronetics electronics were of the order of 0.01% for dead-time corrections, and 0.1% for random coincidences; losses in the scalers were of the order of 1% for 1 count per second.

We have applied radiative corrections deduced from the computations of D. Yennie and N. Meister[7] and assigned an error of 1%.

In the 0° experiments, a correction of the order of 1% due to the finite solid angle and the resultant contribution from charge scattering was applied.

From the experimental cross sections listed in Table I, we have deduced the magnetic form factor. We then fitted the values obtained, assuming the anomalous magnetic moment of the proton to be known from other experiments.

To determine the charge form factors from the 30° data, we computed from the fit the best values of G_m and the errors on these values.

Sachs has shown[1] that in the limit of $q^2 \to 0$, the radii of the charge and magnetic distributions are given by:

$$R = (\text{limit } q^2 \to 0) \sqrt{-6 \frac{dG}{Gdq^2}}$$

Since our data are at sufficiently low q^2, we have used the fits to determine these radii.

V. FORM FACTORS

A. Errors

The values of the magnetic form factors were computed from the experimental cross sections listed in Table I; the values obtained were then fitted by a straight line passing through the point 2.7927 for $q^2 = 0$. The error on the slope of the curve has two sources:

1. The first error is of a random character due to measurement of quantities which are instrinsically random, such as counting rates, or of quantities that have certainly varied between experiments at different q^2, such as the target thickness, the distance between the target and the solid angle slit, the angle and the energy of the recoiling protons, or the efficiency of the SEM.

Errors of this kind are quadratically added and give to each point the error $\Delta_1 G(q_i)$, which is used in the least square fit.

2. There are systematics errors coming from quantities which certainly do not vary between runs, such as the efficiency of the Faraday cup, the area of the target, the area of the slit for the 30° experiment, the value of the standard capacitor of the laboratory, and, for the 0° experiment, the value of the solid angle.

These errors have been quadratically added and contributed 1.1% to the relative error at 0°, and 0.33% for the 30° experiment.

The error on the slope of the straight line due to the second type of error is evaluated by differentiating the least square fit equations and has the value

$$\Delta_2 m = \frac{\Sigma p_i q_i^2 G_i}{\Sigma p_i q_i}$$

We added $\Delta_1 m$ and $\Delta_2 m$ quadratically to obtain the error on the slope.

B. Magnetic Form Factor and Magnetic Radius of the Proton

The cross section is related to G_m by

$$\sigma_{exp} = 2B \left(\frac{P}{P + T} \right)^2 G_m^2 \qquad (3)$$

and, since in our conditions the proton is non-relativistic,

$$\frac{\Delta G_m}{G_m} = \frac{1}{2} \frac{\Delta \sigma}{\sigma}$$

The values of G_m are given in Table I.

The fit of the variations of G_m leads to

$$G_m = 2.7927 - 0.305\ q^2$$

with the errors on the slope,

$$\Delta_1 m = 0.011, \qquad \Delta_2 m = 0.019, \qquad \text{leading to } \Delta m = 0.022$$

The root-mean-square of the magnetic radius of the proton is

$$R_m = 0.810 \pm 0.029 \text{ fermi}$$

The χ^2 test applied to the fit gives a value of five for six degrees of freedom, leading to a probability of a higher χ^2 of 0.40. Thus we think that the treatment of our errors is reasonable.

Our results are shown on Fig. 4 together with results from other groups The central line is our fit and the two dotted lines set limits of one standard deviation from our fit.

In order to compute G_c, we use our fit to obtain the best values of G_m. In the computation of the error on these values, we should again make a distinction between the random and the systematic errors:

$$\Delta_1 G_m = \Delta_1 m \cdot q^2 \qquad \text{(random)}$$

$$\Delta_2 G_m = G_m \cdot 0.01 \qquad \text{(systematic)}$$

For the latter case, only the systematic error on the solid angle at 0° has to be taken into account because the other errors are common to the 0° and 30° experiments.

C. Form Factor of the Charge Distribution

If we consider only the terms in G_c, we can show that the errors on G_c are

$$\frac{\Delta G_c}{G_c} = 0.5 \left(\frac{\Delta T}{T} + \frac{\Delta \sigma}{\sigma} + 4 \cdot \Delta\gamma \right) \qquad (4)$$

$\Delta T/T$ is of the order of 0.01 and the error is mainly due to the statistics, as can be seen from Table I.

The least square fit leads to

$$G_c = 1 - 0.1065\ q^2$$

with

$$\Delta_1 m = 0.0063, \qquad \Delta_2 m = 0.0021, \qquad \text{leading to } \Delta m = 0.0067$$

and to the root-mean-square of the charge distribution

$$R_c = 0.800 \pm 0.025 \text{ fermi}$$

The χ^2 test gives a value of 4.3 for three degrees of freedom, leading to a probability of 0.23 for a higher χ^2.

D. Ratio $G_m/\mu G_c$

Because both G_m and G_c were measured for four values of q^2, we have tried to check the hypothesis $G_m = \mu G_c$, observing that in computing the errors on the ratio, some systematics errors disappear.

The best value for the ratio is $R = 1.0012 \pm 0.0127$; the χ^2 value is 1.16 for three degrees of freedom, corresponding to a probability of 0.75 for higher values; therefore, at the accuracy of our measurements, we cannot reject the hypothesis

$$G_m = \mu G_c \ .$$

VI. CONCLUSIONS

A comparison of our results with those obtained by Lehmann[8] and Drickey[9] shows that the deviations are not significant; the points displaying their measurements are at the limit of the zone corresponding to one standard deviation from our fit, as shown in Figs. 5 and 6. Our values of the form factor

of the distribution of magnetic moment are obtained by direct measurements, which is not the case for the other authors who have had either to combine two observations of the scattered electrons or to assume $\mu_p G_e(q^2) = G_m(q^2)$ to obtain values of G_m for q^2 less than 1 F^{-2}. The accuracy of the determination of the root-mean-square radii was limited by counting rate, and the statistics on the determination of the solid angle.

The value of the root-mean-square radius of the charge distribution (0.80 ± 0.025 fermi) is comparable to the value given by Hand, Miller, and Wilson[2] (0.805 ± 0.011) and in agreement with the Lehmann, Dudelzack, and Sauvage observations (0.82 ± 0.02).[8]

The magnetic radius is found to be 0.810 ± 0.029, with the accuracy comparable to results found by observing the electron.

We point out that the methods used here are very different from the other experiments, this being the main justification for the experiment. It is experimentally very easy to accurately define a solid angle for protons whose range is a few millimeters in brass, and the efficiency of the detection is 100% due to the very good resolution obtained in our counters. In addition, the radiative correction is substantially smaller than when the electron is observed.

ACKNOWLEDGMENTS

We wish to acknowledge help from Professor H. Halban and Professor G. Bishop, who directed us to this subject. We thank Professor A. Blanc-Lapierre for support during this work. Discussions with Professors J. Perez y Jorba, P. Lehmann and J. Lefrancois were very fruitful. V. Round continually found original solutions to our problems. L. Burnod and the accelerator operators provided us with many hours of trouble-free operation.

REFERENCES

1. R. Sachs, Phys. Rev. 126, 2256 (1962).
2. An excellent review of the subject is L. Hand, D. Miller and R. Wilson in Rev. Mod Phys 35, 335 (1963).
3. G. Tautfest and H. Fechter, Rev. Sci. Inst. 26, 229 (1955).
4. D. Frèrejacque and D. Benaksas, Nucl. Inst. 26, 351 (1964).
5. D. Judd, Rev. Sci. Inst. 21, 213 (1950).
6. P. Lehmann, R. Taylor and R. Wilson, Phys. Rev. 126, 1183 (1962).
7. D. Yennie and N. Meister, Phys. Rev. 130, 1210 (1963).
8. P. Lehmann, B. Dudelzach and G. Sauvage, Nuovo Cim. 28, 18 (1963).
9. D. Drickey and L. Hand, Phys. Rev. Letters 9, 521 (1962).

TABLE I

Cross Sections and Form Factors

q^2 (a)	γ	σ_{exp} (b)	$\frac{\Delta\sigma}{\sigma}$%	G_m	ΔG_m	G_c	ΔG_c
0.97	30°	73.53	1.9	-	-	0.877	0.012
0.98	0°	23.97	5.1	2.490	0.063	-	-
1.22	0°	21.96	2.1	2.409	0.025	-	-
1.27	0°	21.00	2.9	2.411	0.034	-	-
1.27	29.6°	57.75	2.0	-	-	0.864	0.016
1.54	0°	19.97	5.0	2.253	0.055	-	-
1.56	0°	17.81	4.0	2.347	0.045	-	-
1.56	30°	49.34	2.2	-	-	0.855	0.017
1.76	0°	19.75	5.9	2.331	0.073	-	-
1.76	29.6°	42.01	3.5	-	-	0.822	0.026

(a) q^2 is in units of fermi^{-2}

(b) σ_{exp} is in units of 10^{-32} cm.

TABLE II

Values of the ratio $p = G_m/\mu G_e$ for different q^2

$q^{2\,(a)}$	p	Δp
0.98	0.984	0.026
1.27	1.000	0.020
1.56	1 018	0.023
1.76	0.986	C.037

(a) q^2 is in units of fermi^{-2}.

LIST OF FIGURES

1. Experimental setup for measurements at 30^{o}.

2. Experimental setup for measurements at 0^{o}. With the spectrometer turned off, the beam entered the Faraday cup.

3. Results of measurements of the proton magnetic form factor at low momentum transfers.

4. Results of measurements of the proton charge form factor at low momentum transfers.

5. Experimental measurements taken at $q^2 = 1.6\ F^{-2}$ and 0^{o}. The dotted curve was used for background subtractions. The solid curve represented the result expected from electron-proton scattering.

6. Experimental measurements taken at 30^{o} and at $1.3\ F^{-2}$.

DOUBLE-FOCUSING SPECTROMETER

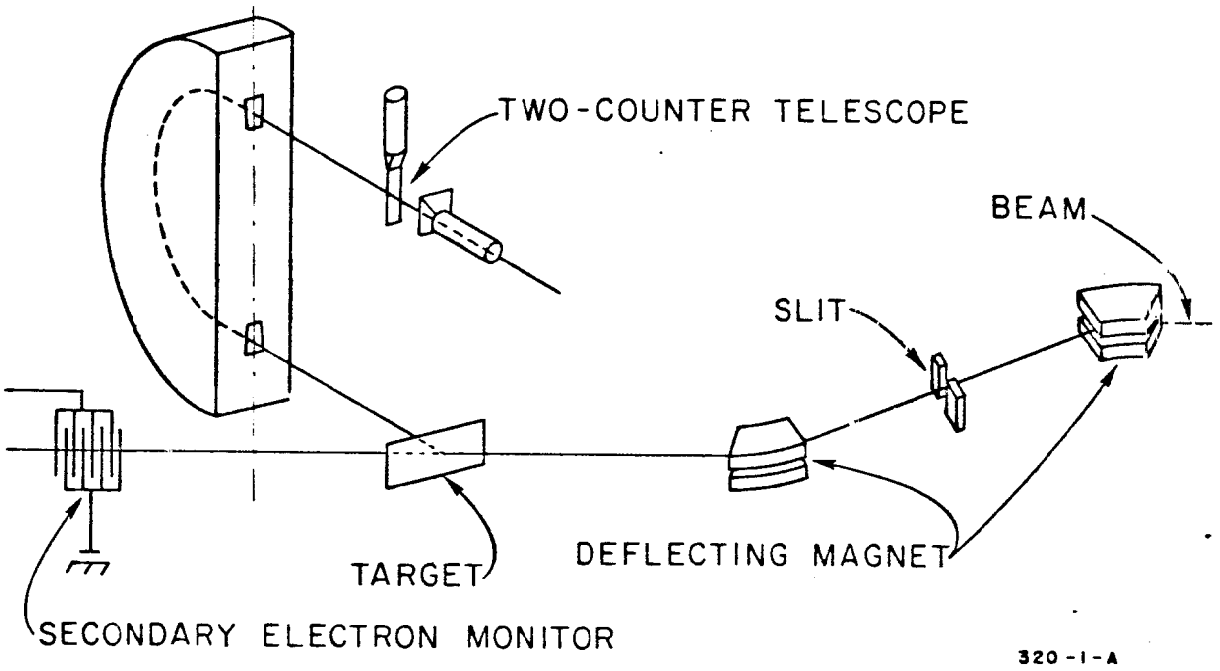

Fig. 1

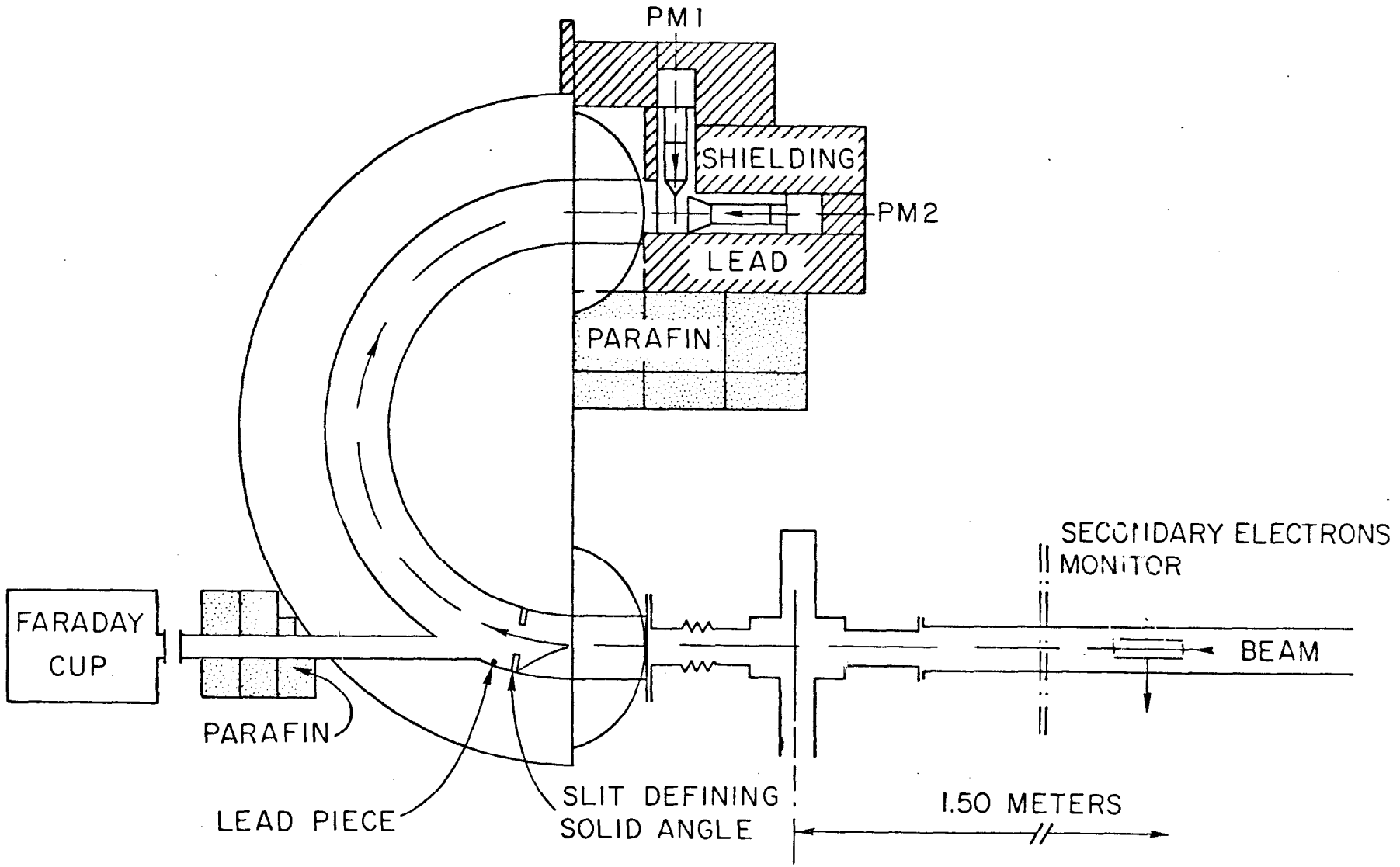
PM1
SHIELDING
PM2
LEAD
PARAFIN
SECONDARY ELECTRONS
MONITOR
FARADAY
CUP
BEAM
PARAFIN
LEAD PIECE
SLIT DEFINING
SOLID ANGLE
1.50 METERS

Fig. 2

320-2-A

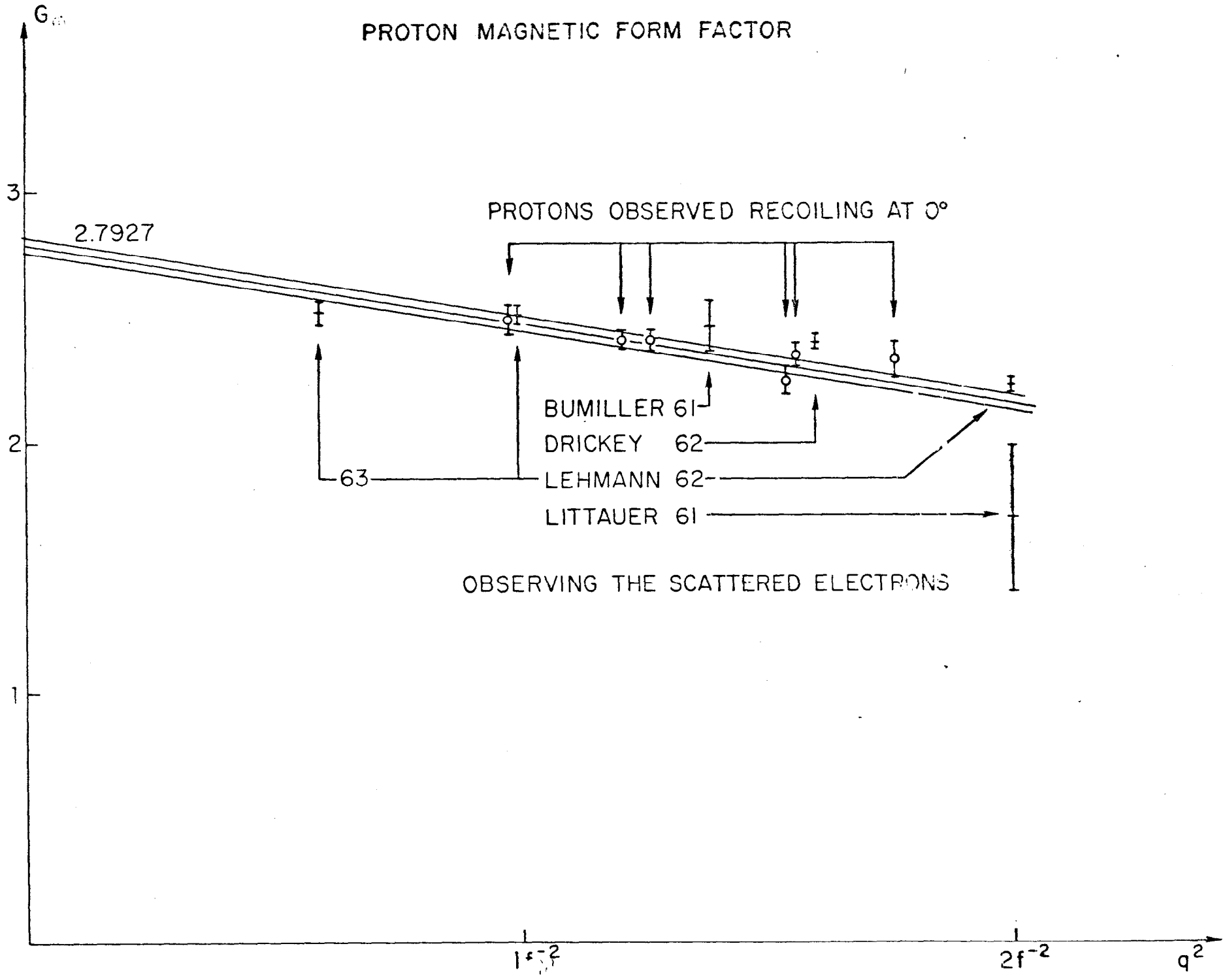
PROTON MAGNETIC FORM FACTOR
G_m
3
2
1
2.7927
PROTONS OBSERVED RECOILING AT 0°
BUMILLER 61
DRICKEY 62
63
LEHMANN 62
LITTAUER 61
OBSERVING THE SCATTERED ELECTRONS
$1f^{-2}$
$2f^{-2}$
q^2

Fig. 3

320-3-A

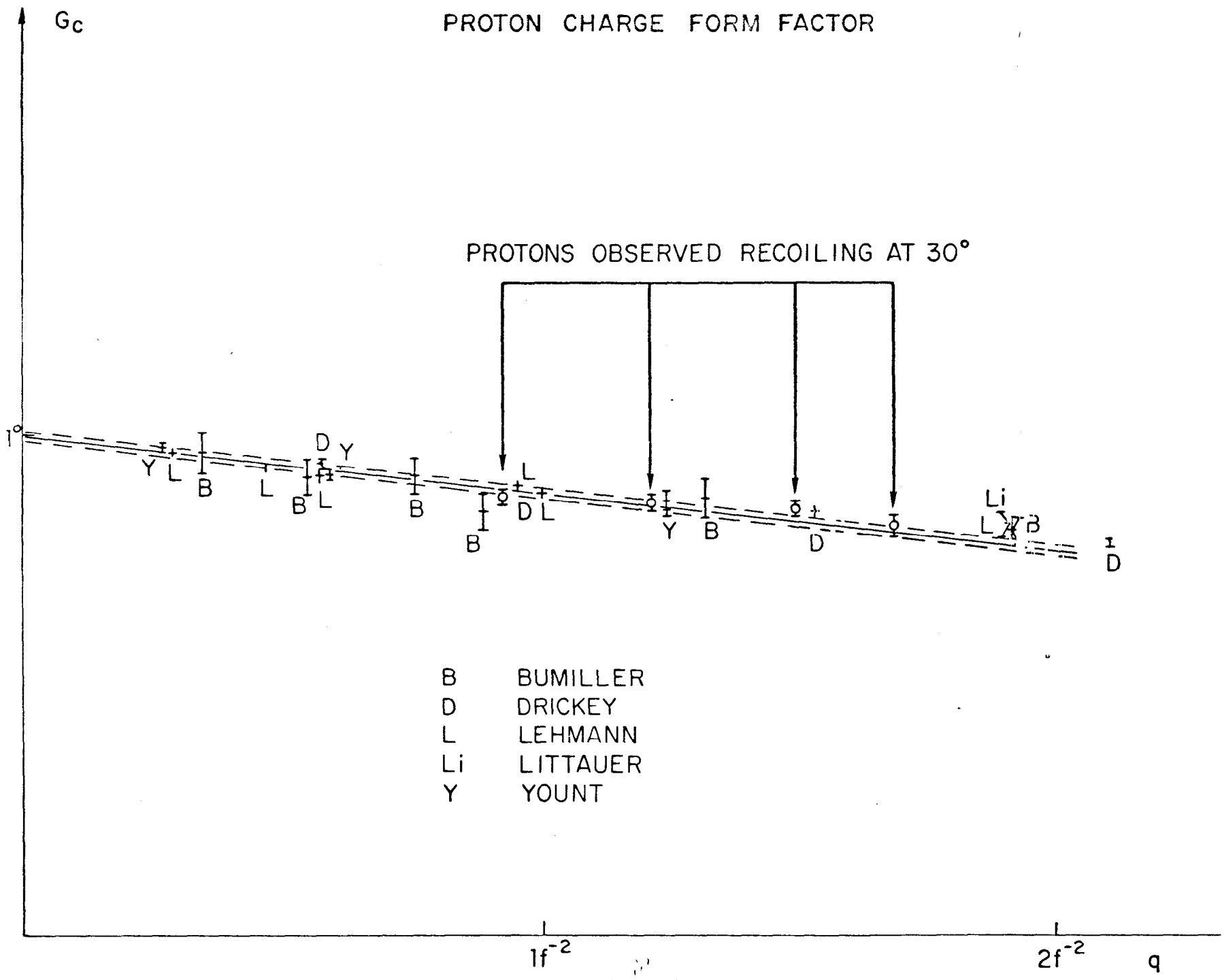
G_C
PROTON CHARGE FORM FACTOR
PROTONS OBSERVED RECOILING AT 30°
1°
B BUMILLER
D DRICKEY
L LEHMANN
Li LITTAUER
Y YOUNT
$1f^{-2}$
$2f^{-2}$
q

Fig. 4

320-4-A

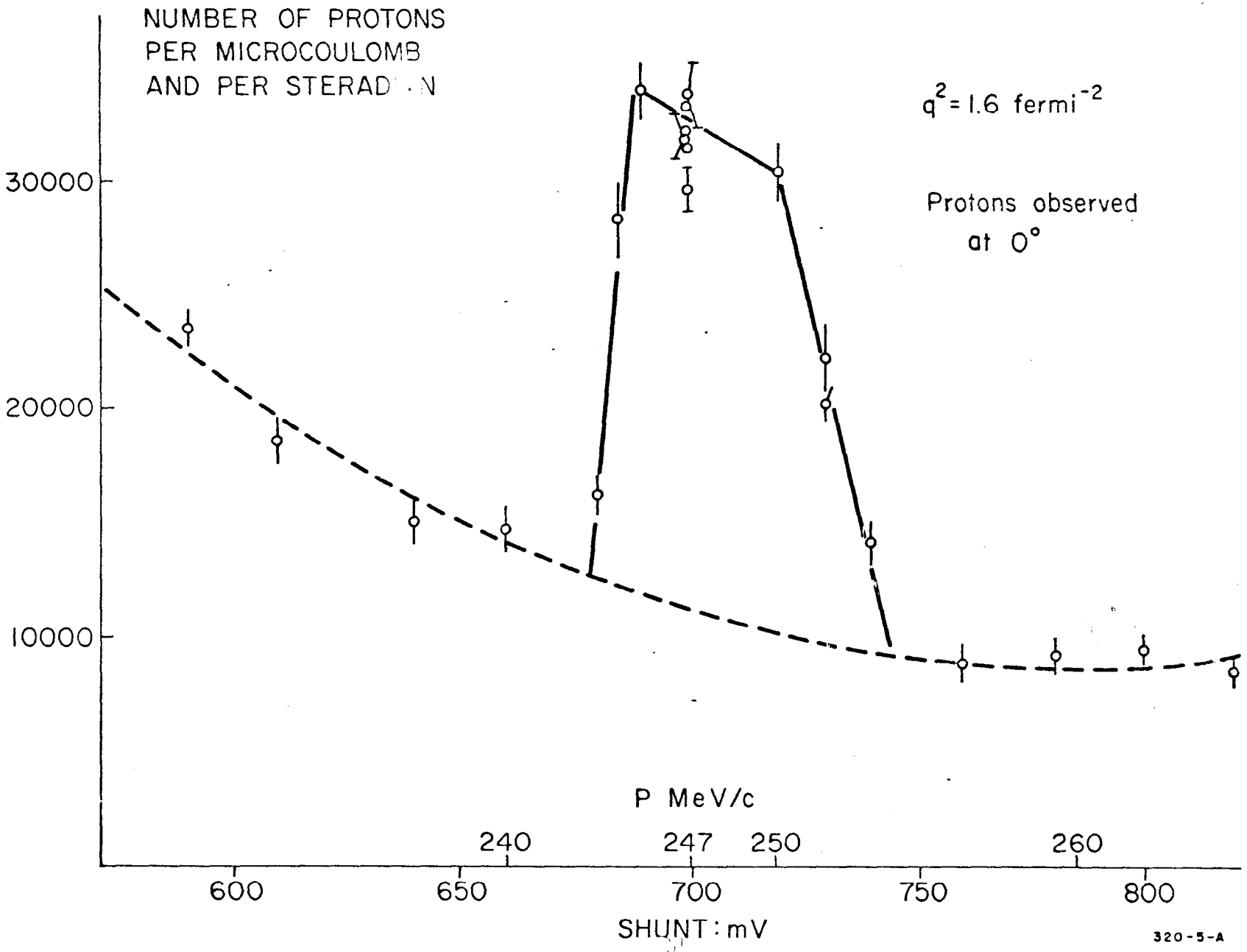
NUMBER OF PROTONS
PER MICROCOULOMB
AND PER STERAD · N
$q^2 = 1.6$ fermi^{-2}
Protons observed
at 0°
30000
20000
10000
P MeV/c
240
247
250
260
600
650
700
750
800
SHUNT : mV
320-5-A

Fig. 5

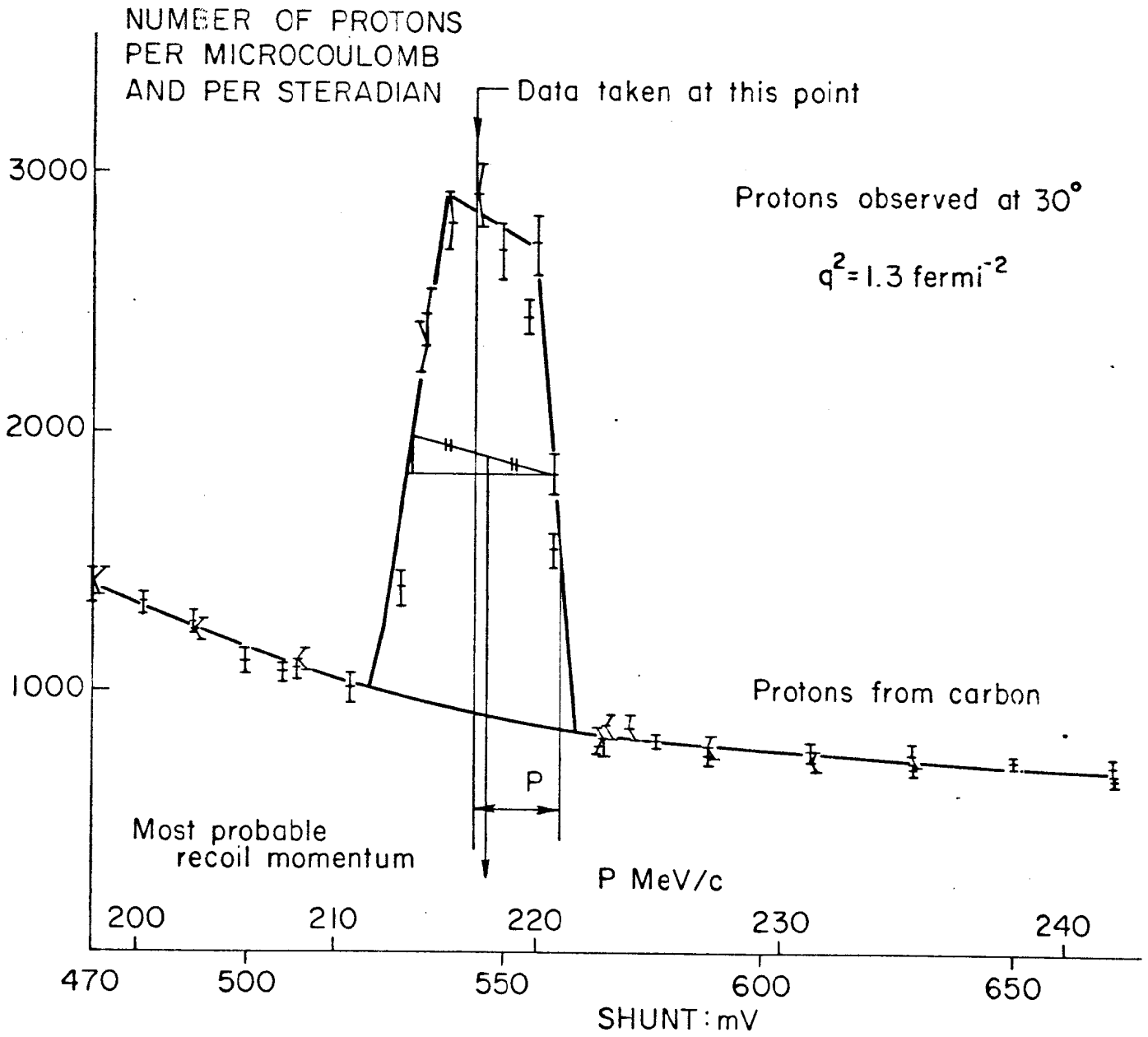
NUMBER OF PROTONS
PER MICROCOULOMB
AND PER STERADIAN
Data taken at this point
3000
2000
1000
Protons observed at 30°
q^2 = 1.3 fermi^{-2}
Protons from carbon
P
Most probable
recoil momentum
P MeV/c
200
210
220
230
240
470
500
550
600
650
SHUNT: mV
320-6-A

Fig. 6